

The influence of boundary heterogeneity in experimental models of mantle convection

A. Namiki and K. Kurita

Department of Earth and Planetary Physics, University of Tokyo, Tokyo, Japan

Abstract. Recent global seismological observations have revealed lateral variations in the thickness of the D'' layer. We have performed laboratory experiments to explore how undulations of various sizes in the D'' layer affect convection patterns. We find that topography on the lower boundary can induce plumes and that there is a critical height above which topography controls convection patterns. Observed undulations in the D'' layer exceed this critical height, suggesting that they may control mantle convection patterns.

Introduction

Recent seismological studies have revealed discontinuous increases in seismic velocities at the top of the D'' layer in many regions around the world, and most models report velocities lower than those of the reference model (PREM) above this discontinuity (e.g., [Lay *et al.*, 1998; Wyssession *et al.*, 1998]). Additionally, lateral variations in the magnitude of this discontinuity, as well mutual inconsistencies between P and S waves, suggest that D'' may not be a simple thermal boundary layer but may also involve chemical heterogeneity [Mériaux *et al.*, 1998]. In such a view, the D'' layer is distinct from the overlying mantle, and the velocity decrease above D'' is interpreted as a thermal boundary layer.

The height of the discontinuity varies laterally from 100 to 450 km above the CMB [Wyssession *et al.*, 1998]. If the top of the D'' layer is the lower boundary of the convecting mantle, then undulations in D'' are expected to control the convection pattern. Both observations and simulations suggest a correlation between these undulations and the convection pattern of the mantle [Wyssession *et al.*, 1998; Montague *et al.*, 1998]. However, there is as yet no quantitative measure of the extent to which such undulations can control mantle dynamics. Here we focus on the role of undulations of the boundary in controlling the spatial and temporal patterns of convection, and we suggest a simple mechanism relating mantle convection to topographical heterogeneities.

Experimental Method

We conducted thermal convection experiments featuring a bump at the lower boundary and observed the temperature fields using thermotropic liquid crystal powder, which changes reflective color within the prescribed temperature range. The experimental tank is rectangular (500 mm long by 30 mm wide) and is filled with fluid to varying depths

(40-74 mm). We adopted this narrow width to obtain an unclouded temperature field. Although the horizontal aspect ratio of the tank is rather small, the convection exhibits three-dimensional patterns at $Ra > 10^6$, because each plume head is smaller than 10 mm. When the Rayleigh number is sufficiently low, convection shows a two-dimensional pattern, which is consistent with previous results [Busse, 1989]. Light passed through a slit illuminates the fluid in cross section, allowing us to observe two-dimensional temperature and flow fields of the three-dimensional convection pattern. The color image is recorded by a video camera.

The tank's side walls are made of 15-mm acrylic plates. The upper and lower boundaries are made of aluminum and copper plates, 3 mm and 2 mm in thickness, respectively. The tank is filled with glycerol solution or silicon oil which is heated from below and cooled from above. The temperatures of the upper and lower boundaries are controlled by circulating water at a precision of $\pm 0.02 \sim 0.1$ °C.

To investigate the effects of boundary topography, we insert a piece of aluminum block (10 mm long by 30 mm wide, 1 ~ 10 mm high) on the lower boundary as an isothermal rigid bump. Prior to insertion, the temperature of the block approximates that of the upper boundary, but it should equilibrate within 1 s to that of the lower boundary.

The Rayleigh number is varied by changing the concentration of glycerol (i.e., kinematic viscosity $8 \times 10^{-6} < \nu < 5 \times 10^{-4} \text{ m}^2\text{s}^{-1}$), the depth of the convecting fluid ($40 < L < 74$ mm), and the temperature difference between the upper and lower boundaries ($4 < \Delta T < 21$ °C). The viscosity of glycerol is temperature-dependent. The maximum viscosity variation in a single experiment is a factor of 2.5. To estimate the Rayleigh number, the viscosity at the central temperature of the convecting layer is adopted. The Prandtl number ($100 < Pr < 5000$) also varies with the concentration of glycerol.

Our experimental setting indicates $Re < 1$. To calculate the Reynolds number, the plume-head radius is selected as a characteristic length scale. The measured plume-head size, rise speed, and kinematic viscosity are $\delta = 3$ mm, $v = 2$ mm s^{-1} , and $\nu = 8.7 \times 10^{-6} \text{ m}^2 \text{ s}^{-1}$, respectively, at $Ra \sim 10^8$. Thus, viscous effects are dominant over inertial effects.

Results

The experiments were carried out at $10^5 < Ra < 10^8$, and two modes of convection were observed. At $Ra \lesssim 10^6$, steady two-dimensional periodic cells are observed: positions of upwelling and downwelling sites are stable. This is interpreted as "steady-state convection". As Ra is increased, the convection pattern becomes unsteady: ascending and descending plumes migrate horizontally with time. We call this "time-dependent convection". These patterns

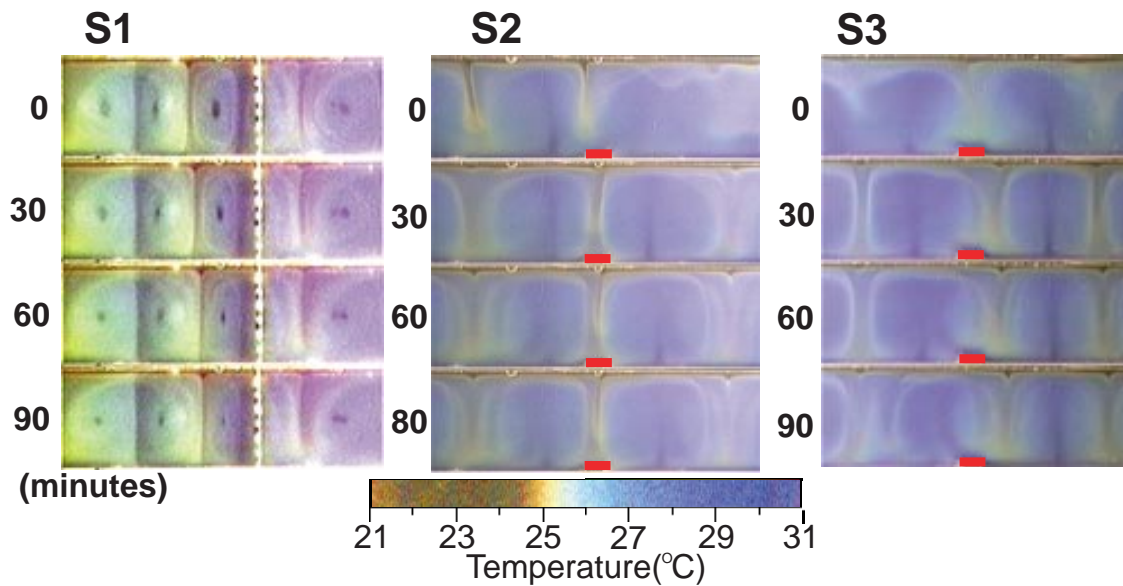


Figure 1. Each panel is a snapshot of the temperature field. Red/yellow areas correspond to low-temperature regions (downwelling sites in convection cell), blue to high-temperature regions (upwellings). S1, S2, and S3 show convection patterns for a homogeneous boundary (without a bump), for a thin bump, and for a thick bump, respectively. For homogeneous case (S1), left-hand numbers indicate time after attaining thermal equilibrium. In remaining panels, numbers indicate time after insertion of a bump, at location shown by red mark. In homogeneous boundary case, steady-state convection is observed. A thin bump does not affect convection patterns, but a thick bump makes a new hot plume and shifts the convection pattern. Line of white beads in S1 is the thermistor array.

are consistent with previous investigations ([Busse, 1989; Weeraratne and Manga, 1998]).

In Fig. 1, S1 shows that the convection under homogeneous boundary conditions is well characterized by stable two-dimensional periodic rolls. Even after long time periods (90 min), the convection pattern in S1 does not show significant variation, and we classify it as a steady-state convection

mode. S3 is the convection pattern in which a thick bump is placed at the site of downwelling after it is confirmed that convection has attained a steady state. Whenever the thick bump is placed at any location, that site always becomes one of upwelling. To see this effect clearly, we intentionally place the bump at a site of steady-state downwelling. We then observe a phenomenon in which the downwelling orig-

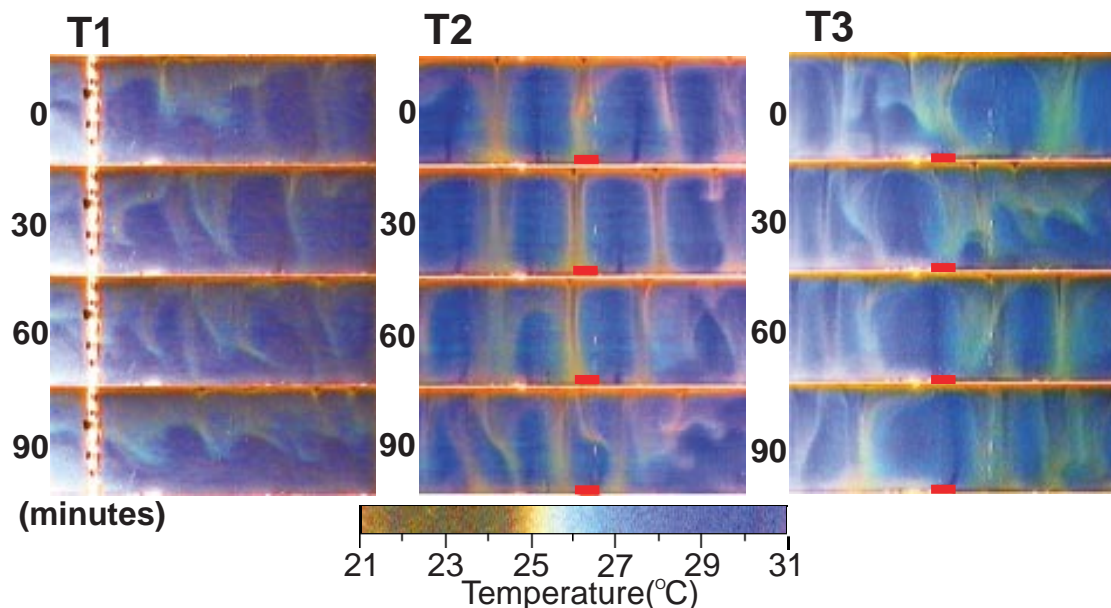


Figure 2. Same as Fig. 1 but for time-dependent convection.

inally located at the site of the bump shifts to the right and a new upwelling originates to the left of the bump. This newly created convection pattern is also steady. On the other hand, the convection pattern for a thin bump, S2, is insensitive to the presence of the heterogeneity.

Fig. 2 shows the temperature fields of convection at $Ra \sim 5 \times 10^6$. T1 shows snapshots of the temperature fields with no bumps, in which ascending and descending plumes migrate laterally and do not reach the upper boundary before disconnection of the plume feeder stem. T2 has a thin bump at the lower boundary, and T3 has a thick bump. In T2 the bump does not affect the turbulent mode, but in T3 the bump generates a steady hot plume and an elongated cell.

These results show that there exists a critical height beyond which thicker bumps modify the initial convection pattern. Fig. 3 summarizes the series of experiments, indicating the relationship between critical bump height and convection patterns. As the Rayleigh number increases, the critical height decreases. It is clear that this critical height scales with the thickness of the thermal boundary layer in the regime of steady state convection. For time-dependent convection, however, a subtle bump – i.e., one which is shorter than the thickness of the thermal boundary layer

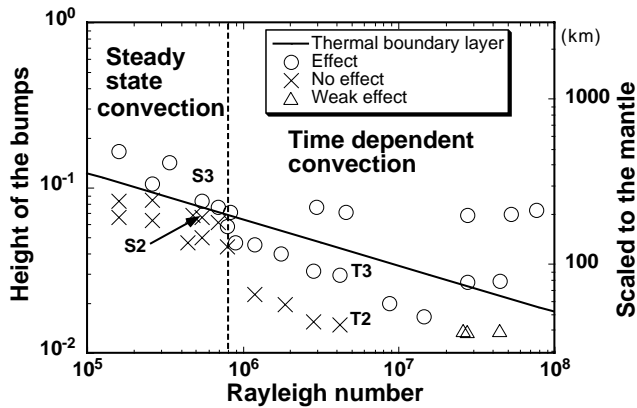


Figure 3. Bump height and thermal boundary layer thickness, normalized by height of convecting layer, versus Rayleigh number. Right y-axis shows corresponding height for Earth’s mantle. Dashed line separates steady-state and time-dependent regimes. ○ denotes case when the bump affects convection pattern; × denotes bump has no effect; △ denotes bump has weak effect. Criteria for these cases are as follows. If bump initiates a new ascending plume, irrespective of initial conditions, even when placed beneath a descending site, it is “effective”. If bump cannot generate a new hot plume, it is “ineffective”. A “weak effect” indicates that although bump makes a hot plume it is not a regular pattern. Solid line indicates calculated thickness of thermal boundary layer following Belmonte *et al.*, [1994], who give $\delta_{th}/l \sim 1/2Nu$ for a wide range of Ra , where l means the height of the convection layer. For $Nu = a * Ra^b$, $a = 0.16$, and $b = 0.281$ [Shen *et al.*, 1996], this yields a quantitative measure of the boundary layer. Attached letters indicate experiments shown in Figs. 1 and 2. This figure demonstrates the existence of a critical height for controlling convection patterns, whose characteristic scale differs between convection modes.

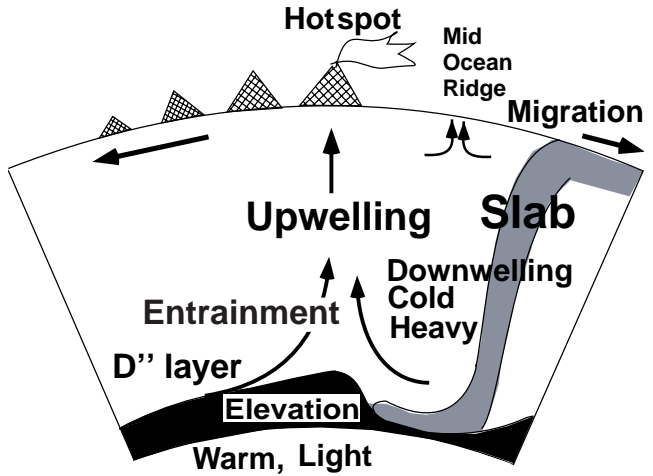


Figure 4. Cartoon of interaction between D’’ layer and mantle convection.

– can control the convection pattern. This result emphasizes importance of the boundary conditions in convection at high Rayleigh numbers.

Discussion

Fig. 3 shows that bumps thicker than the thickness of the boundary layer become the site of steady hot plumes regardless of the previous convection pattern. An almost isothermal bump higher than the boundary layer introduces a high-temperature anomaly above the boundary ($\sim \Delta T/2$), and because the resulting lateral thermal anomaly is unstable it becomes a site of upwelling. At the same time, horizontal flow in the boundary layer is forced upward because of this bump. Because of these coupled effects, the upwelling is strongly fixed at the position of the bump.

Fig. 3 also shows that the scaling law for the critical height differs between the two regimes of convection patterns. The systematically smaller critical height in the regime of time-dependent convection requires further explanation. Time-dependent convection is characterized by fluctuation of the location of plume emanation and by the discontinuous nature of plumes during ascent. Both of these features contribute to decreasing the critical height.

Generation of a new upwelling at the site of a bump placed under a descending plume requires both a shifting of the obstructive descending plume and sufficient buoyancy to generate a new hot plume. In the regime of time-dependent convection, however, the ascending and descending plumes are not anchored, so that a fixed descending plume need not be shifted, in contrast to the case of steady-state convection. Moreover, the thickness of the thermal boundary layer exhibits time dependence at a given location. After the disconnection of the feeder stem, the thermal boundary layer rapidly thins, and a new one gradually grows with a certain time scale. This process produces oscillation in the thickness of the thermal boundary layer, such that there is a minimum thickness of the layer at a given location. To become the seed of the next plume emanation, the bump should be thicker than the minimum thickness of the thermal boundary layer. The critical height is thus smaller than the mean thickness of the thermal boundary layer in the regime of time-dependent convection.

Implications for the Mantle

These experimental results show that a bump of sufficient thickness can fix the location of a hot plume in time-dependent convection. The question remains whether this fixation mechanism operates in the Earth's mantle. Since the Rayleigh number of mantle convection is estimated at about 10^6 to 10^8 , convection in the mantle is expected to be time-dependent.

The first problem is whether the undulations in D'' layer thickness meet the critical height criterion. In Fig. 3 the y -axis at the right is scaled to the thickness of the mantle. The region corresponding to the mantle in the figure is characterized by high sensitivity to topography. Topographical variation whose amplitude exceeds 100 km can affect mantle convection. Since the observed variations in the thickness of the D'' layer reach 340 km [Wysession *et al.*, 1998], undulations in the D'' layer should be sufficient to control the pattern of mantle convection.

The next problem is whether the heterogeneity in D'' matches the bump in our experiments. We consider two models that have been proposed to explain the origin of the D'' layer. One picture suggests that D'' is a dense layer enriched in Fe, because of ongoing differentiation in the outer core and/or reactions between iron alloy in the outer core and silicates in the mantle. In this situation, the thermal conductivity of the D'' layer will be enhanced because of the high content of Fe. Manga and Jeanloz [1996] show that mantle convection can create thickness variations in the D'' layer in this situation, and Montague *et al.* [1998] demonstrate correlation between the thickened regions and the locations of upwellings. Our experiments are analogous to such a situation. The other picture suggests accumulated material from subducted slabs as the source of the D'' layer. Mériaux *et al.* [1998] show that heterogeneity can not simply be explained by thermal anomalies of subducted slabs, so that additional chemical heterogeneities or phase changes are necessary. Wysession [1996] also indicates the correlation between the accumulation of ancient subducted lithosphere and the heterogeneity of seismic velocities in the D'' layer. As cold lithosphere is carried down, it will depress the D'' boundary and displace material within the D'' layer. The warmer, displaced material will elevate the boundary relative to the adjacent cold, subducted material, resulting in boundary topography that is isostatically maintained by the thermal density contrast. In this way, lateral temperature variations and topography are generated simultaneously at same location. Our experimental results show that both effects contribute to the generation of a hot plume. Thus, thickness variations in the D'' layer generated by ancient subducted slab material should generate upwellings above "pile-up" structures.

Consequently, the following picture can be postulated (Fig. 4). Subducted cold slab material depresses the D'' boundary, inducing variations in the thickness of the D'' layer [Montague *et al.*, 1998]. A hot plume then emanates from the edge of the resulting highland, and the relative lo-

cations of hot spots are stabilized by undulations in the D'' layer. Additionally, recent high-pressure experiments and seismic studies suggest the possibility of melting of accumulated material at the base of mantle [Holland and Ahrens, 1997; Williams and Garnero, 1996]. Furthermore, the distribution of ultra-low-velocity zones, which have been interpreted as melting zones, correlate with the locations of hot spots [Williams *et al.*, 1998]. It is expected that the edge of D'' highlands contain partial melt, and melt products entrained in the ascending plume should characterize the geochemical features of hot spots.

Acknowledgments. The authors thank Prof. C. Bina for critical reading and improving the style of this manuscript.

References

- Belmonte, A., A. Tilgner, and A. Libchaber, Temperature and velocity boundary layers in turbulent convection, *Phys. Rev. E*, **50**, 269–279, 1994.
- Busse, F. H., Fundamentals of thermal convection, in *Mantle convection* pp. 23–95. New York; Gordon and Breach Science Publishers, 1989.
- Holland, K. G., and T. J. Ahrens, Melting of $(\text{Mg,Fe})_2\text{SiO}_4$ at the core-mantle boundary of the Earth, *Science*, **275**, 1623–1625, 1997.
- Lay, T., Q. Williams, and E. J. Garnero, The core-mantle boundary layer and deep Earth dynamics, *Nature*, **392**, 461–468, 1998.
- Manga, M., and R. Jeanloz, Implications of a metal-bearing chemical boundary layer in D'' for mantle dynamics, *Geophys. Res. Lett.*, **23**, 3091–3094, 1996.
- Mériaux, C., A. Agnon, and J. Lister, The thermal signature of subducted lithospheric slabs at the core-mantle boundary, *Earth Planet. Sci. Lett.*, **160**, 551–562, 1998.
- Montague, N., L. H. Kellogg, and M. Manga, High Rayleigh number thermo-chemical models of a dense boundary layer in D'' , *Geophys. Res. Lett.*, **25**, 2345–2348, 1998.
- Shen, Y., P. Tong, and K.-Q. Xia, Turbulent convection over rough surfaces, *Phys. Rev. Lett.*, **76**, 908–911, 1996.
- Weeraratne, D., and M. Manga, Transitions in the style of mantle convection at high Rayleigh numbers, *Earth Planet. Sci. Lett.*, **160**, 563–568, 1998.
- Williams, Q., J. Revenaugh, and E. Garnero, A correlation between ultra-low basal velocities in the mantle and hot spots, *Science*, **281**, 546–549, 1998.
- Williams, Q., and E. J. Garnero, Seismic evidence for partial melt at the base of Earth's mantle, *Science*, **273**, 1528–1530, 1996.
- Wysession, M. E., Large-scale structure at the core-mantle boundary from diffracted waves, *Nature*, **382**, 244–248, 1996.
- Wysession, M. E., T. Lay, J. Revenaugh, Q. Williams, E. J. Garnero, R. Jeanloz, and L. H. Kellogg, The D'' discontinuity and its implications, in *The core-mantle boundary region*, edited by M. Gurnis, M. Wysession, B. Buffett, and E. Knittle, pp. 273–297, AGU, Washington, D.C., 1998.

A. Namiki and K. Kurita, Dept. Earth Planet. Phys., University of Tokyo, Tokyo, 113-0033, Japan. (e-mail: namiki@gpsun01.geoph.s.u-tokyo.ac.jp; kurikuri@geoph.s.u-tokyo.ac.jp)

(Received March 8, 1999; revised May 4, 1999; accepted May 12, 1999.)